Design and Analysis of Single Switch Double Enhanced Boost Converter for PV Applications

S.Ramprasath[*], *and C.Krishnakumar*

Saranathan College of Engineering, Department of EEE, Trichy, Tamil Nadu, India

Abstract. This paper presents a systematic and analytical investigation of the non-isolated Single Switch Double Enhanced Boost Converter topology. In simple words combination of a DEC (Double Enhanced Circuit) With an ordinary boost converter. The proposed converter implements the output voltage increasing in geometric progression but with a simpler structure. There is one switch S, n inductors, (n + 2) capacitors, and (2n + 1) diodes in each circuit of the additional series. They also effectively enhance the voltage transfer gain in the power law. Steady-state equations were derived to examine the behaviour of the proposed converter. The proposed converter was designed for 100 W and simulated in MATLAB/Simulink, the simulation results demonstrate its effectiveness in terms of improved efficiency, reduced voltage stress, and enhanced power delivery to the load.

Keywords – Double Enhanced Circuit, Boost Converter, Additional series circuit, Arduino code generator, PWM generator

1 Introduction

The fast expansion of photovoltaic (PV) systems is a result of the rising need for renewable energy sources. These systems harness solar energy and convert it into electrical energy, which can be utilized for various applications. However, the performance and efficiency of PV systems heavily rely on the power conversion stages, particularly the DC-DC converters used for voltage regulation and power conditioning [1-3]. Boost converters are commonly employed in PV applications to step up the low-voltage output from the PV panels to a higher voltage level suitable for the load or energy storage systems. Traditional boost converters have been extensively used due to their simplicity and ease of control. However, they suffer from limitations such as high voltage stress on the components, limited efficiency, and compromised power delivery.

To overcome these limitations, we propose an advanced converter topology that can enhance the performance of PV systems. [4 - 6] One such topology is the single switch double enhanced boost converter. This converter combines the benefits of both the conventional boost converter and the coupled inductor boost converter to improve efficiency, reduce voltage stress, and enhance power delivery. The proposed Single Switch Double Enhanced

* Corresponding author : ramprasath-eee@saranathan.ac.in

Boost Converter is derived from elementary boost converter by adding a DEC (Double Enhanced Circuit) Each circuit of the additional series has one switch S, n inductors, (n + 2) capacitors, and (2n + 1) diodes. This topology allows for increased voltage gain, reduced conduction losses, and improved power delivery to the load. By efficiently utilizing the energy from the PV panels, this converter enables higher efficiency, which is crucial for optimizing the performance of PV systems.

The design and analysis of the single switch double enhanced boost converter involve careful consideration of component selection, inductor design, and control strategy. Various design parameters, such as duty cycle, switching frequency, and coupling coefficient, must be optimized to achieve the desired performance objectives. Additionally, the converter's steady-state characteristics, small-signal behaviour, and control design need to be analysed to ensure stability and effective regulation of the output voltage. In this paper, we present a comprehensive study on the design and analysis of the single switch double enhanced boost converter for PV applications. We discuss the operating principles, design considerations, and control strategy of the converter. Furthermore, we analyse its performance through simulations and experimental validation. The results demonstrate the effectiveness of the proposed converter in improving efficiency, reducing voltage stress, and enhancing power delivery for PV systems.

2 Converter topology and operating principle

2.1 Double enhanced Boost Converter

Figure 1 depicts the proposed (DEBC) converter, which is made up of a single inductor L1 and a single switch S. The Enhanced circuit includes two capacitors (C1 and C11) and two diodes (D1 and D2) that boost the voltage gain. C12 represents the filter capacitor. Each circuit of the additional series has one switch S, n inductors, (n + 2) capacitors, and (2n + 1) diodes. The average output voltage of the converter increases with the number of enhanced circuits added, for design and analysis we consider a single DEC based boost converter.

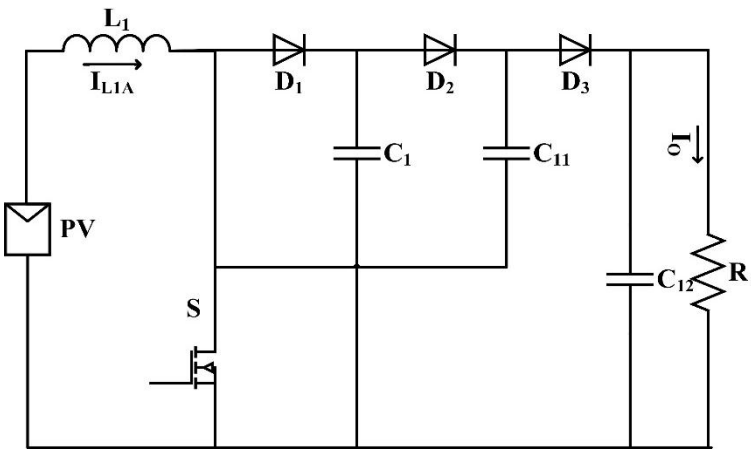

Figure 1. Proposed Double Enhanced Boost Converter

2.2 Operation of Proposed converter

2.2.1 Mode 1

Figure 2 shows the schematic for mode 1 operation. At t = 0, $V_{C1} = V_{C11} = Vin$. When S is turned ON, the inductor gets charged through switch S to Vin. The load current Io is supply by Capacitor C12.

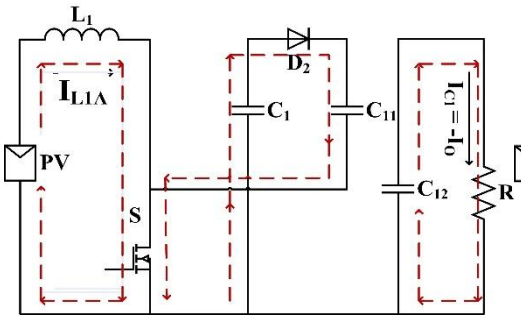

Figure 2. Mode 1 (S = ON)

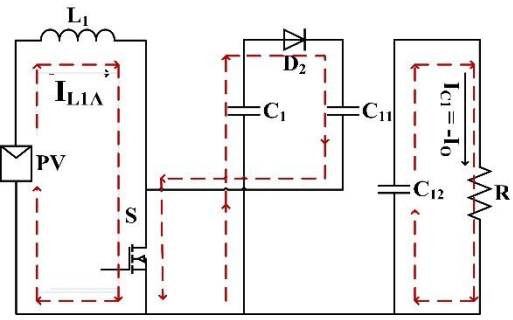

Figure 3. Mode 2 (S = OFF)

The steady state equations for Mode 1 are

$$V_{C1} = V_{C11} = V_1 \tag{1}$$

$$V_{in} = V_L$$

$$\frac{di_L}{dt} = \frac{V_{in}}{L} \tag{2}$$

$$i_{C12} = -i_0$$

$$\frac{dV_{C12}}{dt} = -\frac{V_0}{RC_{12}} \tag{3}$$

$$i_{C1} = -i_{C11}$$

$$\frac{dV_{C1}}{dt} = -\frac{C_{11}}{C_1} \times \frac{dV_{C11}}{dt} \tag{4}$$

2.2.2 Mode 2

Figure 3 shows the schematic for mode 2 operation. At t = Ton, $V_{C1} = V_{in} + V_L$. When S if turned OFF, the stored charge in inductor L and Input voltage Vin charges the C_1 Capacitor. The load current Io and Capacitor C_{12} is supplied by Capacitor C_{11}.

The steady state equations for Mode 2 are

$$V_{in} + V_L = V_{C1}$$

$$\frac{di_L}{dt} = \frac{V_1}{L} - \frac{V_{in}}{L} \tag{5}$$

$$\frac{dV_{C1}}{dt} = \frac{i_L}{C_1} - \left(\frac{C_1}{C_{11}} \times \frac{dV_{C11}}{dt}\right) \tag{6}$$

$$\frac{dV_0}{dt} = \left(\frac{C_{11}}{C_{12}} \times \frac{dV_{C11}}{dt}\right) - \frac{V_0}{RC_{12}} \tag{7}$$

2.2.3 Steady State Analysis of proposed converter

Using equation (1) to (7) the steady state design equation for proposed converter was derived. As per the volt-sec balance rule, the net charge stored in the inductor is zero. Equating the voltage across inductor for one cycle to zero, the average output voltage was derived.

$$V_{in}D(T_s) = V_1(1-D)T_s - V_{in}(1-D)T_s$$

$$V_1 = \frac{V_{in}}{(1-D)} \tag{8}$$

V_{C1} & V_{C11} are changed to V_1 , hence voltage across C_{12} is changed to $2V_1 = V_0$.
The Average output voltage Vo,

$$V_0 = 2V_1 = \frac{2V_{in}}{(1-D)} \tag{9}$$

The input current $I_S = I_L$, For Ideal Converter $V_{in}I_L = V_0 I_0$

$$V_{in}I_L = \left(\frac{2}{1-D}\right)V_{in}I_0$$

$$I_L = I_0\left(\frac{2}{1-D}\right) \tag{10}$$

To find L, the Ripple Current (ΔI_L)
From (1), $(di_L / dt) = (V_{in} / L)$

$$\Delta I_L = \left(\frac{V_{in}}{L \times f}\right) \tag{11}$$

ΔV_0 (Ripple Output Voltage)

$$\Delta q = |-I_0| * DT_s$$

$$\Delta q = \frac{V_0}{R} \times \frac{D}{f}$$

$$\frac{\Delta q}{C_{12}} = \frac{V_0 \times D}{R \times f \times C_{12}}$$

$$\Delta V_0 = \frac{V_0 \times D}{R \times f \times C_{12}} \tag{12}$$

Average State Equation for proposed converter are

$$\frac{di_L}{dt} = \frac{V_{in}}{L} + \left(\frac{V_1}{L} \times (1-D)\right)$$

$$\frac{dV_{C1}}{dt} = \left(-\frac{C_{11}}{C_1} \times \frac{dV_{C11}}{dt}\right) + \left(i_L \times \frac{(1-D)}{C_1}\right)$$

$$\frac{dV_{C11}}{dt} = \left(-\frac{C_1}{C_{11}} \times \frac{dV_{C1}}{dt}\right) + \left(i_L \times \frac{(1-D)}{C_{11}}\right)$$

$$dV_0 / dt = \left(\frac{C_{11}}{C_{12}} \times \frac{dV_{C11}}{dt} \times D\right) - \frac{V_0}{RC_{12}}$$

3 Design Consideration

The proposed converter was designed for the specification listed in table 1.

Table I. Specifications

Parameters	Values
Input Voltage Vs	18 V
Output voltage V0	60 V
Power P	100 W
Inductor Current ripple ΔIL	5 % of IL_{avg}
Output voltage ripple ΔV_0	5% of Vo
Frequency f	5 KHz

The design parameters are calculated using a MATLAB m-file. The m-file is executed in MATLAB to obtain the design parameter. Figure 4, Shows the design parameters for the proposed converter. The simulation of suggested converter was done for the findings received from the mfile in figure 4.

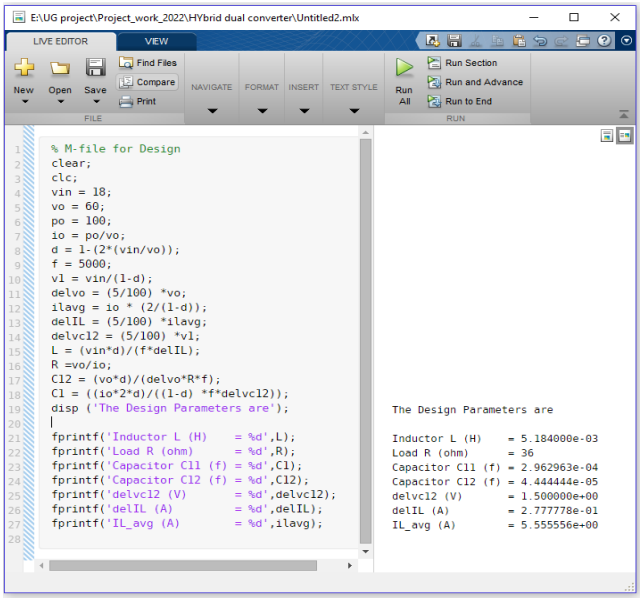

Figure 4. Design parameters for proposed converter

4 Simulation and Hardware results

For the specifications shown in Figure 3, the suggested converter was simulated in MATLAB. The simulation result validated the obtained design equations. The proposed converter was simulated using a single 100 W Photo voltaic (PV) module as the source and uses the Perturb and observe algorithm to track the maximum power point for a step change in irradiation [7-10].

Figure 5a illustrates the proposed converter's simulation circuit. Figure 5b, which displays the voltage across the inductor, verified the 0.28 A ripple in the inductor current. The capacitor current I_{C2} and voltage V_{C2} was shown in figure 5c. The output voltage V_O and output current I_O for the DEBC shown in figure 5d. The Voltage V_{PV} and Current I_{PV} of a 100W PV panel are shown in Figure 5e.

The changes in Duty ratio d and output power P_O for a step change in irradiance are shown in Figures 5f and 5g. At t=2.5 seconds, the irradiance was changed from 1000 W/m2 to 800 W/m2. The simulation results we received were good, and the outcomes are consistent with the proposed design.

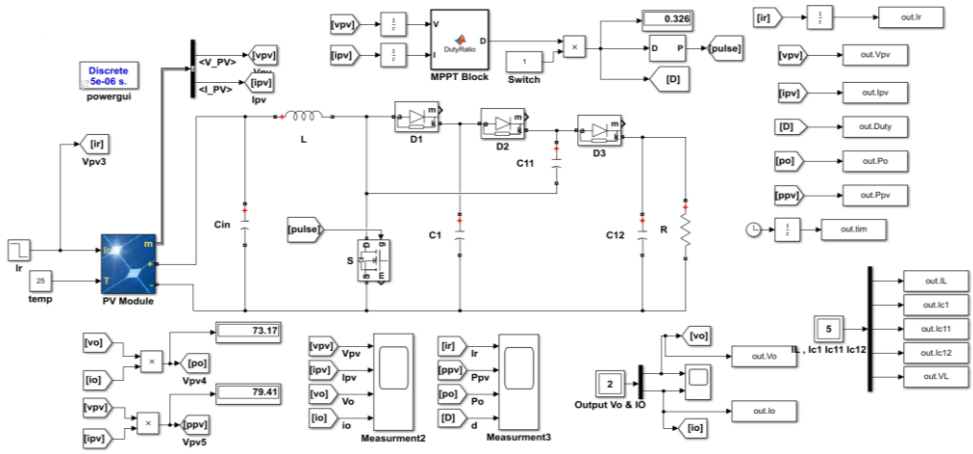

Figure 5a. Simulation of Proposed DEBC

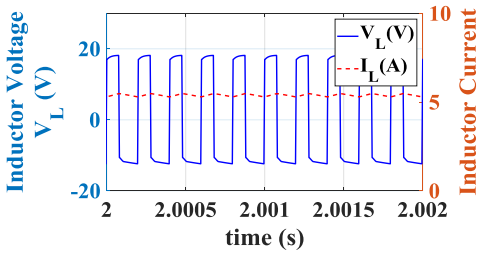

Figure 5b. Inductor Voltage V_L and Current I_L

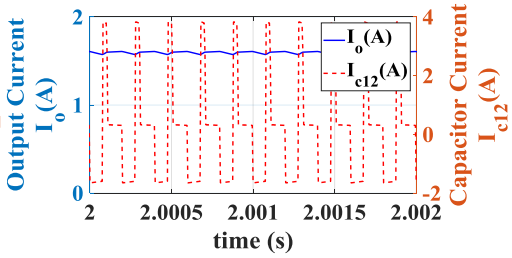

Figure 5c. Voltage V_{C12} and Current I_O

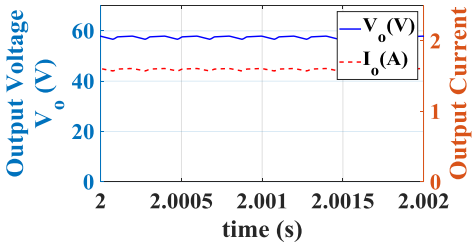

Figure 5d. Output Voltage V_O and Current I_L

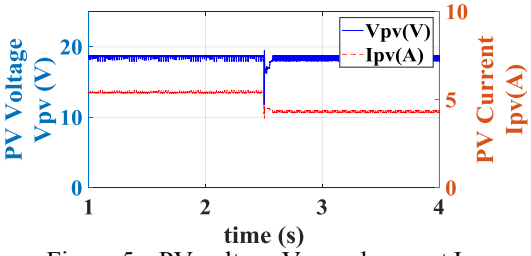

Figure 5e. PV voltage V_{PV} and current I_{PV}

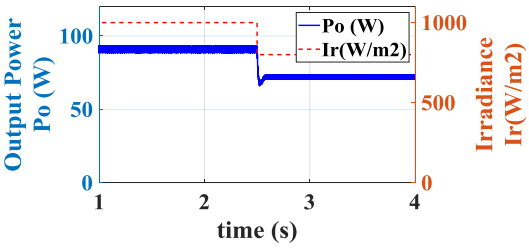

Figure 5d. Output Power P_O and Irradiance

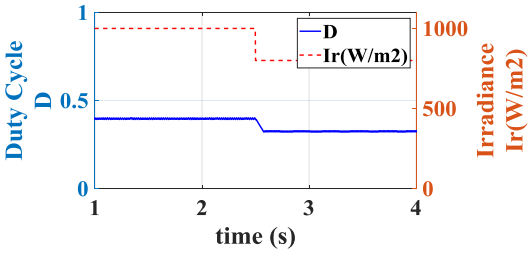

Figure 5e. Duty Ratio D and Irradiance

4.1 Software implementation

The 8-bit Arduino ATmega2560 is appropriate for the MATLAB/Simulink environment. It has a 10-bit ADC resolution and an 8-bit PWM resolution. The ATmega2560 is used within the suggested model to connect with Simulink and to supply the converter for Simulink-generated pulses. The Simulink Support Package for Arduino Hardware offers a simple method for developing code that utilize Simulink blocks that support Arduino and can be included in your Simulink model. [11-13] The blocks are used to configure the associated analog pin and PWM pins, as well as to read and write data to them. The PV voltage and current are measured using the analog pins on the Arduino A0 and A1 and the measured data are passed on to MATLAB to obtain the precise duty ratio for the applied irradiance.

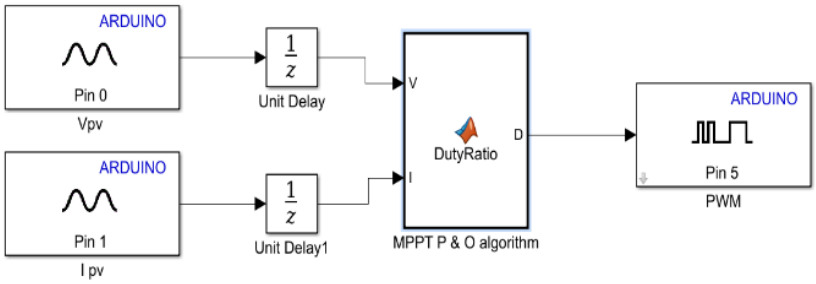

Figure 6. Code generation using MATLAB

Figure 6 shows the Simulink diagram for code generator using Arduino hardware support package. The analog pin A0 measures the voltage Vpv, and A1 measures the current Ipv of PV panel. The P&O algorithm was written in mfile in the function block which gave appropriate duty ration for varying irradiance. The PWM pin 5 is selected to provide the duty ratio.

4.2 Hardware implementation

To configure and run the model on compatible Arduino hardware, follow these instructions:

- Make use of a USB cable to connect the Arduino board to your computer.
- To access the Configuration Parameters dialogue in the Simulink model, select Simulation > Model Configuration Parameters.
- From the Hardware board parameter list, choose the Hardware Implementation pane and then the Arduino hardware you need.
- Choose Run on board under external mode in the Hardware tab of the Simulink model. and then click Build, Deploy & Start. The linked Arduino hardware will now get the Simulink model.
- To drive the suggested converter, connect to the MOSFET driver while using DSO to observe the PWM pulse.
- Simulink models should be saved.

Figure 7 depicts the hardware layout for the proposed converter. The system was divided into four modules: the power circuit, the MOSFET driver module, the Arduino controller, and the sensing module. Figure 7a depicts a pulse created at a frequency of 7 KHz; the waveform captured after diver therefore has an amplitude of 12 V. Figure 7b depicts

the inductor current I_L, which increases when the switch is turned on and decreases from I_{Lmax} to I_{Lmin} when the switch is turned off. Figure 7c represents the output voltage V_{C2} and the voltage across capacitor C_1 (V_{C1}). The hardware results confirm the DEBC's higher voltage gain. The observed output voltage exceeds the levels attained with classical boost. Hardware testing and measurements support the theoretical design and analysis, proving the converter's anticipated benefits and advantages.

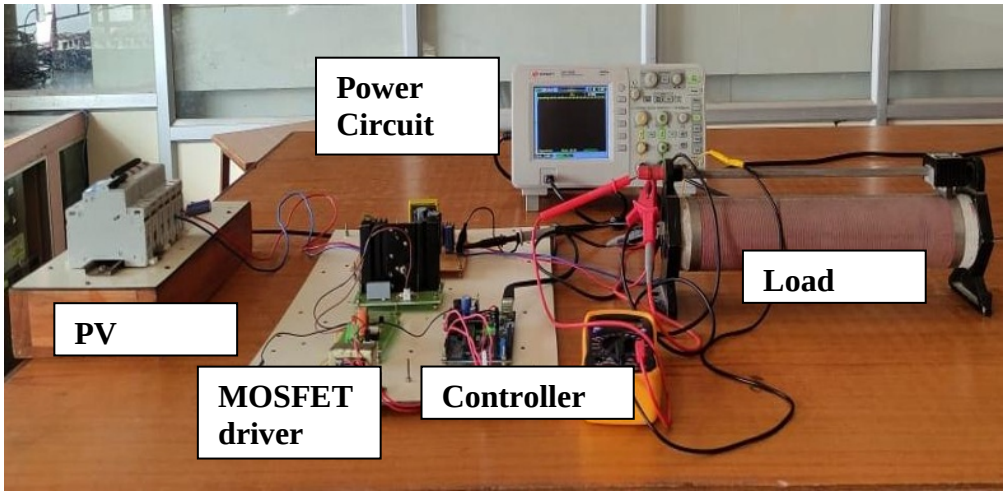

Figure 7. Hardware arrangement of Proposed DEBC

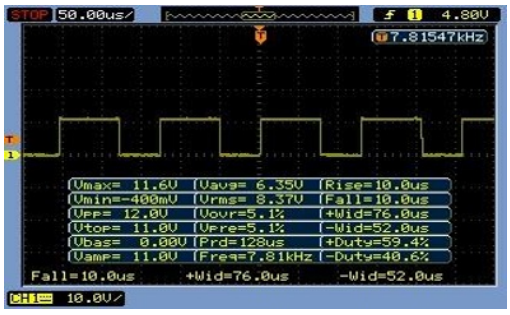

Figure 7a. Triggering Pulse for Switch S

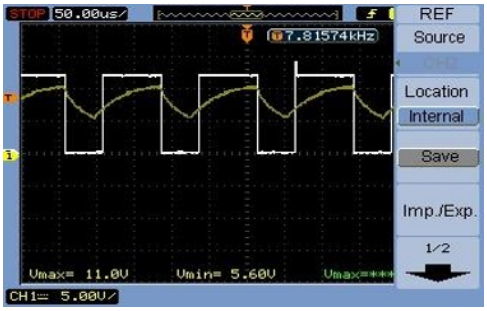

Figure 7b. Inductor Current I_L

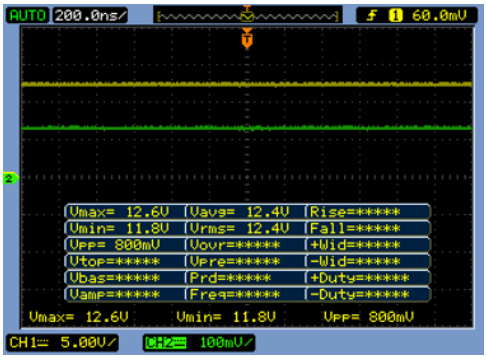

Figure 7c. Voltage across capacitor C_1

Figure 7d. Voltage across capacitor C_{12} and C_{11}

5 Conclusion

In this article, the single switch double enhanced DC-DC boost converter setup is extended to the Solar PV panel to produce the desired output. The various building blocks of the proposed system were designed and simulated in the MATLAB/Simulink environment. The code generation was done in Arduino based hardware support package in MATLAB. Overall, the Single Switch Double Enhanced Boost Converter for PV Applications design and analysis offer a reliable and effective solution for increasing power extraction from PV panels. It is a desirable option for many different PV system designs due to its higher voltage gain, increased efficiency, decreased component stress, and better voltage regulation.

References

1. M. Veerachary and P. Sen, "Dual-Switch Enhanced Gain Boost DC–DC Converters," in IEEE Transactions on Industry Applications, vol. 58, no. 4, pp. 4903-4913, July-Aug. 2022, doi: 10.1109/TIA.2022.3171533.
2. D. Huang, J. Pan, P. Luo, D. Yang and H. Ji, "An Improved Dual Switches Quadratic Boost DCDC Converter," 2021 IEEE 2nd China International Youth Conference on Electrical Engineering (CIYCEE), Chengdu, China, 2021, pp. 1-6, doi: 10.1109/CIYCEE53554.2021.9676837.
3. M. Veerachary and P. Sen, "Design and Analysis of Dual-switch Enhanced Gain Boost Converter," 2020 IEEE International Conference on Computing, Power and Communication Technologies (GUCON), Greater Noida, India, 2020, pp. 83-89, doi: 10.1109/GUCON48875.2020.9231176.
4. H. Bi, P. Wang and Y. Che, "A Capacitor Clamped H-Type Boost DC-DC Converter With Wide Voltage-Gain Range for Fuel Cell Vehicles," in IEEE Transactions on Vehicular Technology, vol. 68, no. 1, pp. 276-290, Jan. 2019, doi: 10.1109/TVT.2018.2884890.
5. M. -K. Nguyen, T. -D. Duong and Y. -C. Lim, "Switched-Capacitor-Based Dual-Switch High-Boost DC–DC Converter," in IEEE Transactions on Power Electronics, vol. 33, no. 5, pp. 4181-4189, May 2018, doi: 10.1109/TPEL.2017.2719040.
6. G. Zhang et al., "A Generalized Additional Voltage Pumping Solution for High-Step-Up Converters," in IEEE Transactions on Power Electronics, vol. 34, no. 7, pp. 6456-6467, July 2019, doi: 10.1109/TPEL.2018.2874006.
7. D. G. Kumar, A. Ganesh, D. S. N. M. Rao, N. V. Sireesha, R. K. Gatla and S. Saravanan, "Grid Integration of Photovoltaic System with a Single-Phase Reduced Switch Multilevel Inverter Topology," 2022 IEEE 2nd International Conference on Sustainable Energy and Future Electric Transportation (SeFeT), Hyderabad, India, 2022, pp. 1-6, doi: 10.1109/SeFeT55524.2022.9909189.
8. Mansour AS, Zaky MS. A new extended single-switch high gain DC-DC boost converter for renewable energy applications. Sci Rep. 2023 Jan 6;13(1):264. doi: 10.1038/s41598-022-26660-7. PMID: 36609658; PMCID: PMC9823105.
9. Erickson, R.W. (2007). DC–DC Power Converters. In Wiley Encyclopedia of Electrical and Electronics Engineering, J.G. Webster. https://doi.org/10.1002/047134608X.W5808.pub2
10. Kim, S.; Jung, H.; Lee, S.-h. Modified Design of Two-Switch Buck-Boost Converter to Improve Power Efficiency Using Fewer Conduction Components. *Appl. Sci.* **2023**, *13*, 343. https://doi.org/10.3390/app13010343.
11. G. Oltean, V. Oltean and H. A. Balea, "Method for Rapid Development of Arduino-based Applications Enclosing ANN," IECON 2019 - 45th Annual Conference of the

IEEE Industrial Electronics Society, Lisbon, Portugal, 2019, pp. 138-143, doi: 10.1109/IECON.2019.8927573.

12. S. P. Biswas, M. K. Hosain, M. R. I. Sheikh, M. F. Kibria, F. Hasan and M. Y. -Y. U. Haque, "A Noble Approach for Generating Real Time Firing Pulse for Inverter Using Arduino and MATLAB/Simulink," 2018 4th International Conference on Electrical Engineering and Information & Communication Technology (iCEEiCT), Dhaka, Bangladesh, 2018, pp. 662-665, doi: 10.1109/CEEICT.2018.8628042.
13. S. P. Biswas, M. K. Hosain, M. W. Rahman, M. H. Mondol and P. Mazumder, "Real-Time Hardware-in-the-Loop Simulator Based Triggering Pulse Generator for Single Phase Inverter," 2018 International Conference on Advancement in Electrical and Electronic Engineering (ICAEEE), Gazipur, Bangladesh, 2018, pp. 1-4, doi: 10.1109/ICAEEE.2018.8643009.